

Supplementary Information

Section S1: Characterization of Ce-NiFe-LDHs

X-ray diffraction (XRD) measurements were conducted to explore the crystallinity and phase composition of as-prepared samples on a Rigaku D/MAX-2550 diffractometer using Cu-K α radiation ($\lambda = 0.15418$ nm). The morphology and size of 3D Ce-NiFe-LDHs were examined by field emission scanning electron microscope (FESEM/EDS, ZEISS Ultra Plus) using an accelerating voltage of 15 kV. The morphology and lattice of 3D Ce-NiFe-LDH were examined by field emission transmission electron microscopy (Japan-JEOL-JEM 2100 F) using an accelerating voltage of 200 kV. X-ray photoelectron spectroscopic (XPS) measurement of 3D Ce-NiFe-LDHs was performed by VG Multilab 2000 to examine the elemental composition and chemical state. The FT-IR measurements were using the AVATAR 360 spectrometer (Nicolet instrument Corporation, America) in the region 4000-500 cm^{-1} . All binding energies were calibrated with the saturated hydrocarbon C 1s peak at 284.5 eV. The specific surface area was tested by the Brunauer-Emmett-Teller (BET) model. The active species were certified by using an Electron Spin Resonance (ESR, Bruker A200). Electrochemical tests were performed at an electrochemical workstation (CHI 660E, CH Instruments Inc, Shanghai, China) using Na₂SO₄ (0.1 M) as an electrolyte and a three-electrode system (working electrode: CC/Ce-NiFe-LDHs material; opposite electrode: carbon rod, reference electrode: Hg/HgO electrode).

Section S2: UPLC/MS test conditions

This test was performed on an ACQUITY UPLC BEH C18 column using the UPLC-MS system $\mu\text{m } 2.1 \times 50$ mm and a quadrupole time-of-flight mass spectrometer (Waters Synapt G2, USA), including ESI electrospray ion source. Mobile phase A is acetonitrile, and mobile phase B is 0.1% formic acid. Use binary mobile phase at a flow rate of 0.3 mL/min. The mobile phase gradient is set to A=5% (0 min), 17% (5 min), 30% (7 min), 85% (11 min), 100% (13 min), 5% (14 min), and 5% (20 min). The injection volume is 5.0 μL . The identification of products is based on retention time and mass spectrometry. The capillary voltage is 3.0 kV, the cone hole voltage is 40 V, and the extraction cone voltage is 4.0 V. The ion source temperature and solvent removal temperature are 373 K and 623 K, respectively. The gas velocity in the conical hole is 50 L/h, and the solvent gas removal rate is 700 L/h. The full scan quality range is 100 to 1000 m/z.

Section S3: Test method for H₂O₂ consumption

The iodometric method was used to test H₂O₂. Fluorescence reagents (0.1 M potassium hydrogen phthalate and 0.4 M potassium iodide aqueous solution) were typically complexed with the reaction system in a specific volume. The H₂O₂ concentration was determined during each reaction phase by measuring the absorbance at 220 nm with a UV-Vis spectrophotometer. The H₂O₂ breakdown tests were carried out in an 'O₂' saturated, visible light-irradiated environment. In the Quartz tube, 30 mg of catalyst was suspended in 50 mL of H₂O₂ aqueous solution (10 mM). The apparatus was then exposed to visible light for 90 min before measuring the remaining H₂O₂ concentration.

Section S4: Test method for cyclic experiment

Using xenon lamp to simulate sunlight as a light source, add 30 mg catalyst into a beaker containing 50 mL 30 mg/L tetracycline solution, place the beaker in a magnetic stirrer and stir for 30 min to reach adsorption equilibrium, turn on the light source, add the corresponding amount of H₂O₂ to start the degradation experiment and time. The 3 mL samples were taken from the beaker at a specific time point, filtered by 0.22 μm filter membrane, and the absorbance was measured by ultraviolet spectrophotometer. After the reaction, the corresponding volume of tetracycline was added to the beaker and mixed evenly, so that the concentration of the TC-HCl in the beaker was maintained at 30 mg/L, and then H₂O₂ was added to the solution to start the degradation experiment, which was repeated for six times. Each group of experiments was carried out three times to ensure the accuracy of experimental data.

Section S5: Germination and growth test of soybean

In order to explore the effects of different solutions on the germination and growth of soybean seeds, soybean seeds with developmental potential were selected as experimental materials. The experimental design consisted of three treatment groups: a control group (TC-HCl), a blank group (pure water), and a treatment group (a solution after a specific treatment). The experimental procedure is as follows:

1. Place the selected soybean seeds in a pre-treatment environment, cover the seeds with a towel soaked in different solutions, ensure that the solution is evenly distributed, and place in a darkroom to simulate the conditions of germination without

light.

2. Regularly observe and record the number of germination of seeds in each group until the preset germination standard is reached.
3. After removing the towel, completely immerse the roots of the germinated seeds in the corresponding solution and transfer them to a well-lit growing environment.
4. Irrigate the plants in each group daily with the same solution for the following experimental cycles to ensure consistency of experimental conditions.
5. On the third and fifth days of the experiment, the growth status of each group of plants was photographed in the main view and top view, and the plant height was accurately measured as the main index to evaluate the growth performance.

Table S1 Molecular information of TC-HCl, OTC, FT and NPX

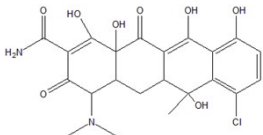
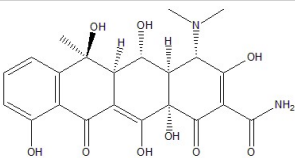
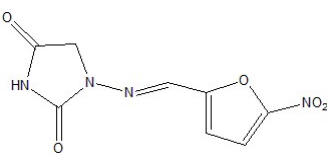
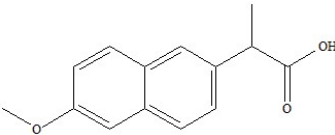
antibiotic	Molecular formula	Structure chart	Wave length (nm)
TC-HCl	$C_{22}H_{24}N_2O_8$		358
OTC	$C_{22}H_{24}O_9N_2$		355
NFT	$C_8H_6N_4O_5$		367
NPX	$C_{14}H_{14}O_3$		262

Table S2 Specific surface area and average pore size of NiFe-LDHs, NiCe-LDHs and Ce_x-NiFe-LDHs.

	NiFe-LDHs	NiCe-LDHs	Ce _{0.5} -NiFe-LDHs	Ce ₁ -NiFe-LDHs	Ce ₂ -NiFe-LDHs
Specific surface area (m ² /g)	8.79	9.88	22	42	40
Average pore size (nm)	4.528	4.834	6.698	3.444	3.622

Table S3 Comparison of the present research with similar studies done before.

Material	Light source	Pollutant	Dosage of	Time(min)	R (100%)	Ref.
			catalyst			
Cds@NiFe-LDH	vis-light ($\lambda \geq 400$ nm)	Caffeine	0.5 g/L	120 min	66%	[3]
Ag-CN/SnS ₂	500 W Xe lamp	TC	0.2 g/L	150 min	94.9%	[4]
FePcS-PMA-LDH	500 W Xe lamp	BPA	40 mg	120 min	100%	[5]
ND/CuFe-LDH	500 W Xe lamp	MB	0.0667 g/L	120 min	93.5%	[6]
M ₃ Cr-CO ₃ -LDH	150 W halogen lamp	MB	0.5 g	140 min	90.67	[7]
MnMgFe-LDH	UV-vis-light	MB	0.0667 g/L	300 min	92%	[8]
NiFeCe-LDH	500 W Xe lamp	TC	30 mg	60 min	100%	This Work

Table S4 Change of metal ion content before and after reaction

sample	Relative content					
	Ni 2p		Fe 2p		Ce 3d	
	Ni ²⁺	Ni ³⁺	Fe ²⁺	Fe ³⁺	Ce ³⁺	Ce ⁴⁺
Before reaction NiFeCe-LDHs(%)	39.36	60.64	26.49	51.84	33.15	23.19
After reaction NiFeCe-LDHs(%)	34.05	66.65	39.97	38.72	16.37	36.04

Table S5 Cost estimation of catalyst and system in actual practice.

Items	1m ³ cost	Notes
Chemical raw (Cost _{raw})	91.29 ¥/m ³ experimental consumption and wholesale costs	94.65 ¥/m ³ for 4 runs ²
Electricity & Energy (Cost _{EE})	3.36 ¥/m ³	23.67 ¥/m ³
H ₂ O ₂ (Cost _{H₂O₂})	4.56 ¥/m ³ wholesale costs	4.56 ¥/m ³
Cost _{raw} + Cost _{EE} + Cost _{H₂O₂}		28.32 ¥/m ³

Table S6 condensed Fukui functions and condensed dual descriptors

Atom	q(N)	q(N+1)	q(N-1)	CDD
1(C)	-0.0261	-0.0729	0.0075	0.0132
2(C)	-0.0649	-0.0856	0.0028	-0.047
3(C)	-0.0033	-0.0227	0.0165	-0.0003
4(C)	-0.0444	-0.0521	-0.0066	-0.0302
5(C)	0.0985	0.0754	0.1409	-0.0194
6(C)	-0.0551	-0.085	-0.0071	-0.0182
7(C)	0.0862	0.0845	0.0883	-0.0003
8(C)	-0.0184	-0.0211	-0.0147	-0.0009
9(C)	-0.0401	-0.0578	-0.0077	-0.0147
10(C)	0.136	0.078	0.1446	0.0493
11(C)	-0.0503	-0.0539	-0.0476	0.0009
12(C)	-0.0239	-0.0252	-0.0226	0

13(C)	0.0662	0.0574	0.0722	0.0029
14(C)	0.0901	0.0598	0.1209	-0.0004
15(C)	0.0261	0.0202	0.0286	0.0034
16(C)	0.1372	0.0809	0.148	0.0455
17(C)	-0.0636	-0.0816	-0.0552	0.0097
18(C)	0.1358	0.0865	0.1423	0.0429
19(C)	0.1511	0.1436	0.1748	-0.0162
20(C)	-0.0909	-0.0969	-0.0844	-0.0005
21(O)	-0.1869	-0.2181	-0.1029	-0.0528
22(O)	-0.2158	-0.2786	-0.1934	0.0403
23(O)	-0.1755	-0.1983	-0.1431	-0.0096
24(O)	-0.2077	-0.2619	-0.1902	0.0367
25(O)	-0.2018	-0.2259	-0.1845	0.0068
26(O)	-0.2123	-0.2168	-0.2015	-0.0062
27(O)	-0.3185	-0.3465	-0.2255	-0.065
28(N)	-0.1487	-0.1622	-0.1191	-0.0161
29(N)	-0.0625	-0.0655	-0.0593	-0.0002
30(C)	-0.0336	-0.0409	-0.0296	0.0033
31(C)	-0.0389	-0.0439	-0.0355	0.0017
32(O)	-0.1267	-0.1719	-0.1096	0.0281
33(H)	0.0447	0.0177	0.0709	0.0008
34(H)	0.033	0.017	0.0607	-0.0118

35(H)	0.0466	0.0246	0.0745	-0.0059
36(H)	0.0296	0.0192	0.0411	-0.0012
37(H)	0.031	0.0258	0.0351	0.0011
38(H)	0.0293	0.0172	0.0388	0.0026
39(H)	0.0344	0.0253	0.0399	0.0037
40(H)	0.0455	0.0289	0.0517	0.0104
41(H)	0.0317	0.0209	0.0405	0.002
42(H)	0.0327	0.0246	0.0411	-0.0002
43(H)	0.0318	0.0242	0.0436	-0.0043
44(H)	0.1148	0.1036	0.1339	-0.0079
45(H)	0.1236	0.1114	0.1357	0.0001
46(H)	0.1452	0.132	0.154	0.0044
47(H)	0.1499	0.139	0.1588	0.002
48(H)	0.1249	0.1059	0.1454	-0.0014
49(H)	0.0926	0.0863	0.1061	-0.0072
50(H)	0.026	0.0204	0.0276	0.0041
51(H)	0.0415	0.0274	0.0519	0.0037
52(H)	0.0379	0.03	0.0419	0.0039
53(H)	0.0268	0.0214	0.0292	0.0031
54(H)	0.0365	0.0351	0.0373	0.0006
55(H)	0.0379	0.023	0.0487	0.0042
56(H)	0.1348	0.1184	0.1446	0.0066

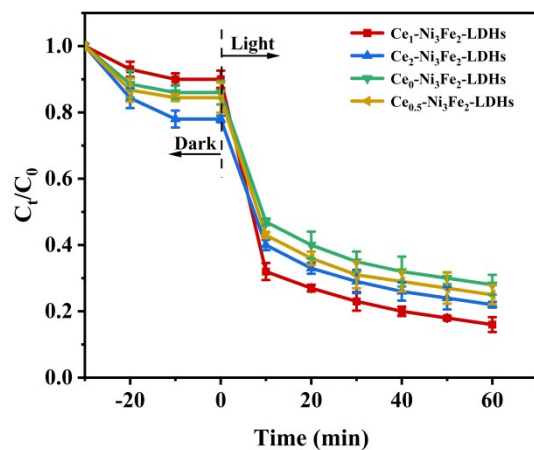


Fig. S1 Effect of Ce-doping amount on TC-HCl removal rate.

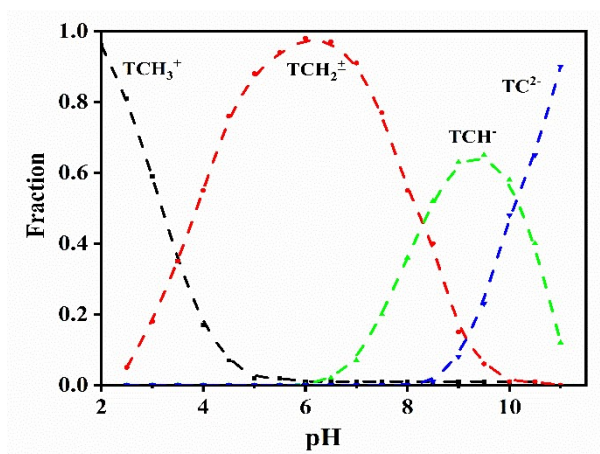


Fig. S2 The morphology of TC-HCl at different pH

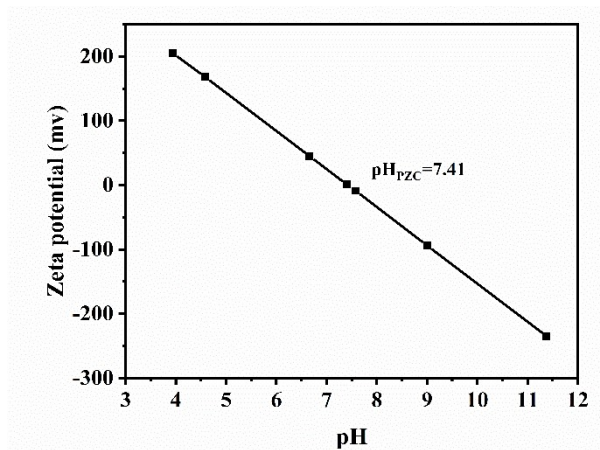


Fig. S3 Isoelectric point of Ce-NiFe-LDHs

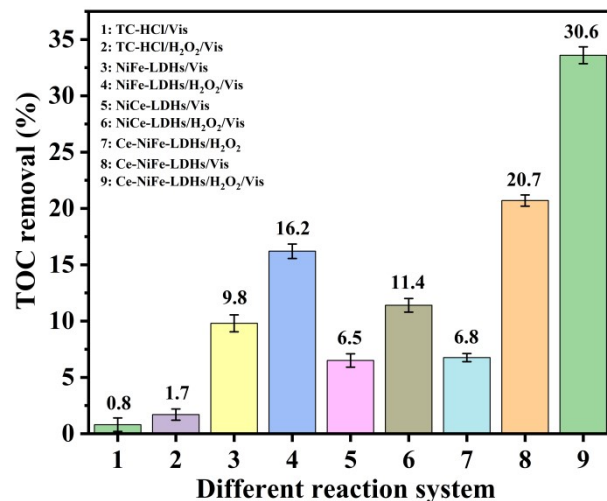


Fig. S4 TOC removal rate of TC-HCl in different reaction systems.

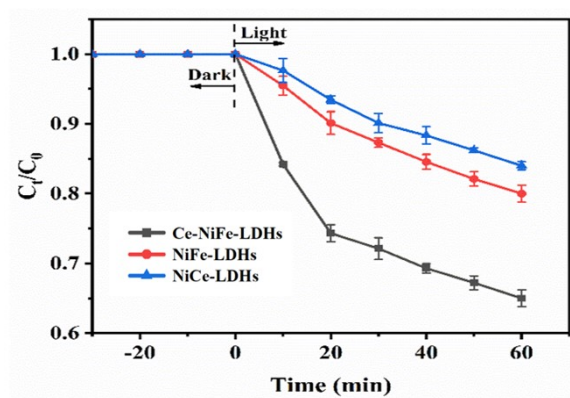


Fig. S5 Consumption of H₂O₂

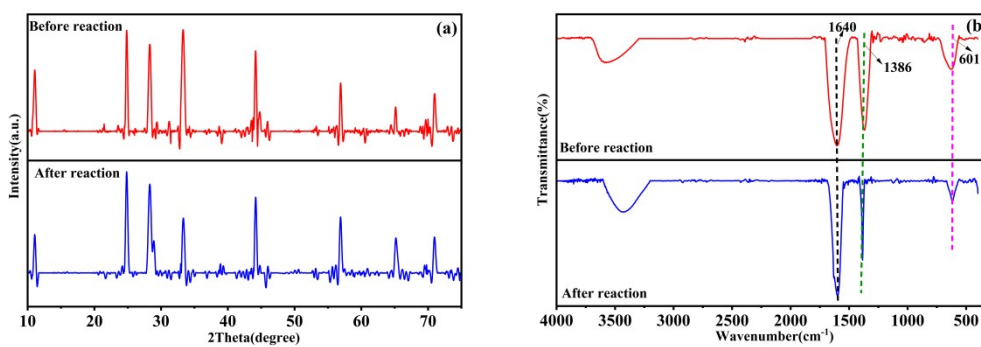


Fig. S6 Pre- and post-reaction (a) XRD, (b) FT-IR of Ce-NiFe-LDHs.

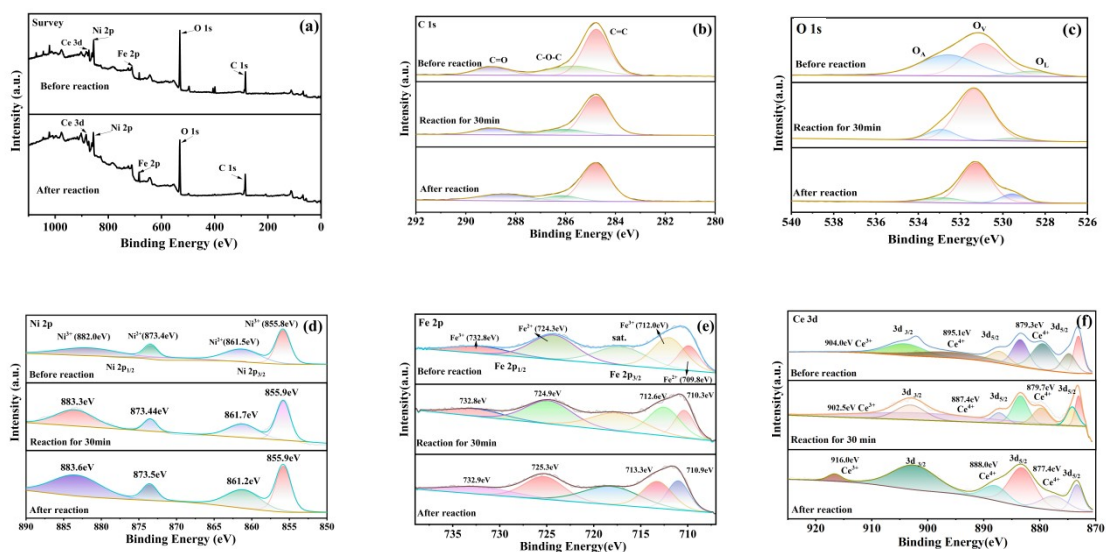


Fig. S7 XPS spectrum of Ce-NiFe-LDHs before, reaction 30 min and after reaction: (a) XPS survey spectra, (b) C 1s, (c) O 1s, (d) Ni 2p, (e) Fe 2p, (f) Ce 3d.

Reference:

- [1] Qing Xin, Siqi Liu, Shixu Lu, Surface-bound sulfate radical-dominated degradation of sulfamethoxazole in the CuFeAl-LDH/peroxymonosulfate system: The abundant hydroxyl groups enhancing efficiency mechanism, *Chem. Eng. J.* 471 (2023) 144453.
- [2] Fu-Xue Wang, Zi-Wei Zhang, Zi-Chen Zhang, Prussian blue analogue nanospheres immobilized on self-floating biochar for micropollutant degradation via photo-Fenton process, *Chem. Eng. J.* 487 (2024) 150506.
- [3] B. Fang, Z. Xing, M. Guo and Y. Qiu, Phosphorus-doping CdS@NiFe layered double hydroxide as Z-Scheme heterojunction for enhanced photocatalytic and photo-fenton degradation performance, *Sep. Purif. Technol.* 274 (2021) 119066.
- [4] W. Zhao, Y. Li, P. Zhao, L. Zhang, B. Dai, J. Xu, H. Huang, Y. He, D.Y. Leung, Novel Z-scheme Ag-C₃N₄/SnS₂ plasmonic heterojunction photocatalyst for degradation of tetracycline and H₂ production, *Chem. Eng. J.* 405 (2021) 126555.
- [5] F. Huang, S Tian, Y Qi, E Li, L Zhou and Y Qiu, Synthesis of FePcS-PMA-LDH Intercalation Composite with Enhanced Visible Light Photo-Fenton Catalytic Activity for BPA Degradation at Circumneutral pH, *Materials.* 13(8) (2020) 1951.
- [6] L. Liu, S. Li and Y. An, Hybridization of Nanodiamond and CuFe-LDH as Heterogeneous Photoactivator for Visible-Light Driven Photo-Fenton Reaction: Photocatalytic Activity and Mechanism, *Catalysts.* 9(2) (2019) 118.
- [7] G. Pan, M. Xu, K. Zhou and Y. Meng, Photocatalytic Degradation of Methylene Blue Over Layered Double Hydroxides Using Various Divalent Metal Ions, *Clays Clay Miner.* 67 (2019) 340-347.

- [8] R.G.L. Gonçalves, H. M. Mendes and S. L. Bastos, Fenton-like degradation of methylene blue using Mg/Fe and MnMg/Fe layered double hydroxides as reusable catalysts, *Appl. Clay Sci.* 187 (2020) 105477.